Published in : Inorganic Chemistry (2021), vol. 60, n°21, pp. 16666-16677
DOI: 10.1021/acs.inorgchem.1c02568
Status : Postprint (Author's version)

FUNCTIONALIZATION OF MONO- AND BIMETALLIC MIL-100(AL,FE) MOFS BY ETHYLENEDIAMINE: POSTFUNCTIONALIZATION, BRØNSTED ACIDO-BASICITY, AND UNUSUAL CO_2 SORPTION BEHAVIOR

Timothy Steenhaut*, Luca Fusaro, Koen Robeyns, Séraphin Lacour, Xiao Li, Julien G. Mahy, Véronique Louppe, Nicolas Grégoire, Gabriella Barozzino-Consiglio, Jean-François Statsyns, Carmela Aprile, Yaroslav Filinchuk*, Sophie Hermans*

Luca Fusaro - Namur Institute of Structured Matter (NISM), UNamur, Rue de Bruxelles 61, B-5000 Namur, Belgium

Koen Robeyns - Institute of Condensed Matter and Nanosciences (IMCN), UCLouvain, Place Louis Pasteur 1/L4.01.03, 1348 Louvain-la-Neuve, Belgium; https://orcid.org/0000-0002-4763-4217

Séraphin Lacour - Institute of Condensed Matter and Nanosciences (IMCN), UCLouvain, Place Louis Pasteur 1/L4.01.03, 1348 Louvain-la-Neuve, Belgium

Xiao Li - Institute of Condensed Matter and Nanosciences (IMCN), UCLouvain, Place Louis Pasteur 1/L4.01.03, 1348 Louvain-la-Neuve, Belgium

Julien G. Mahy - Institute of Condensed Matter and Nanosciences (IMCN), UCLouvain, Place Louis Pasteur 1/L4.01.03, 1348 Louvain-la-Neuve, Belgium; https://orcid.org/0000-0003-2281-9626

Véronique Louppe - Institute of Condensed Matter and Nanosciences (IMCN), UCLouvain, Place Louis Pasteur 1/L4.01.03, 1348 Louvain-la-Neuve, Belgium

Nicolas Grégoire - Institute of Condensed Matter and Nanosciences (IMCN), UCLouvain, Place Louis Pasteur 1/L4.01.03, 1348 Louvain-la-Neuve, Belgium

Gabriella Barozzino-Consiglio - Institute of Condensed Matter and Nanosciences (IMCN), UCLouvain, Place Louis Pasteur 1/L4.01.03, 1348 Louvain-la-Neuve, Belgium

Jean-François Statsyns - Institute of Condensed Matter and Nanosciences (IMCN), UCLouvain, Place Louis Pasteur 1/L4.01.03, 1348 Louvain-la-Neuve, Belgium

Carmela Aprile - Namur Institute of Structured Matter (NISM), UNamur, Rue de Bruxelles 61, B-5000 Namur, Belgium https://orcid.org/0000-0002-3193-3239

CORRESPONDING AUTHORS

Timothy Steenhaut - Institute of Condensed Matter and Nanosciences (IMCN), UCLouvain, Place Louis Pasteur 1/L4.01.03, 1348 Louvain-la-Neuve, Belgium; https://orcid.org/0000-0003-2881-9440;

Email: timothy.steenhaut@uclouvain.be

Published in : Inorganic Chemistry (2021), vol. 60, n°21, pp. 16666-16677
DOI: 10.1021/acs.inorgchem.1c02568
Status : Postprint (Author's version)

Yaroslav Filinchuk - Institute of Condensed Matter and Nanosciences (IMCN), UCLouvain, Place Louis Pasteur 1/L4.01.03, 1348 Louvain-la-Neuve, Belgium; https://orcid.org/0000-0002-6146-3696;
Email: yaroslav.filinchuk@uclouvain.be
Sophie Hermans - Institute of Condensed Matter and Nanosciences (IMCN), UCLouvain, Place Louis Pasteur 1/L4.01.03, 1348 Louvain-la-Neuve, Belgium; https://orcid.org/0000-0003-4715-7964;
Email: sophie.hermans@uclouvain.be

ABSTRACT

The metal sites of MIL-100(Fe), MIL-100(Fe,Al), and MIL-100(Al) metal–organic frameworks (MOFs) were decorated with ethylenediamine (EN). Interestingly, the Al-containing MOFs presented hierarchized porosity, and their structural integrity was maintained upon functionalization. Solution and solid-state NMR confirmed the grafting efficiency in the case of MIL-100(Al) and the presence of a free amine group. It was shown that MIL-100(Al) can be functionalized by only one EN molecule in each trimeric Al_3O cluster unit, whereas the other two aluminum sites are occupied by a hydroxyl and a water molecule. The $-NH_2$ sites of the grafted ethylenediamine can be used for further postfunctionalization through amine chemistry and are responsible for the basicity of the functionalized material as well as increased affinity for CO_2. Furthermore, the presence of coordinated water molecules on the Al-MOF is responsible for simultaneous Brønsted acidity. Finally, the Al-containing MOFs show an unusual carbon dioxide sorption mechanism at high pressures that distinguishes those materials from their iron and chromium counterparts and is suspected to be due to the presence of polarized Al–OH bonds.

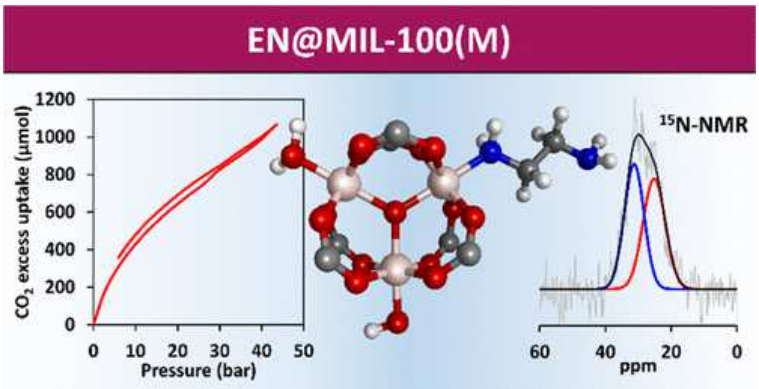

KEYWORDS: AMINES -- FUNCTIONALIZATION -- MATERIALS -- METAL ORGANIC FRAMEWORKS -- MOLECULES

Published in : Inorganic Chemistry (2021), vol. 60, n°21, pp. 16666-16677
DOI: 10.1021/acs.inorgchem.1c02568
Status : Postprint (Author's version)

Introduction

Metal–organic frameworks (MOFs) are porous coordination polymers that hold great promise in fields such as the capture of greenhouse gases, (1) including carbon dioxide, (2) gas storage for energy applications (H_2, CH_4), (3) drug delivery, (4) sensing, (5) and catalysis. To improve the sorption of CO_2 and other guest molecules in MOFs, functionalization of those materials with basic functions, (6) and more specifically amines, (7) is very efficient. Such functions are also very valuable tools for postfunctionalization purposes relying on the rich chemistry of amines, (8) as well as for base-promoted catalysis. (9) The incorporation of amines is usually carried out using modified linkers to build the MOF. However, amine-bearing linkers are often more expensive. One alternative is to functionalize metal sites in MOFs with cheap ethylenediamine (EN) (10−14) or other polyamines, (15) which use one $-NH_2$ site as an anchor to the MOF's structure, leaving a second pendant amine site available. The chromium-based MIL-100(Cr), built using the benzene-1,3,5-tricarboxylate (also called trimesate, BTC^{3-}) ligand, is a MOF that has shown great promise in this perspective. (16−18) However, this chromium-based MOF is not likely to be used in large-scale industrial applications due to environmental and health concerns. (19) This is because of strong regulations concerning chromium, which is highly hazardous in its +VI oxidation state. (20) Nevertheless, the MIL-100 structure remains very interesting for functionalization purposes because its large pores (25 and 29 Å diameters) allow for introducing functional units while still maintaining high surface areas. (21,22) For this reason, we investigated the possibility to functionalize MIL-100(Al) and MIL-100(Fe), which are based on widely available (and thus cheap) and less problematic metals, as well as their bimetallic counterpart MIL-100(Fe,Al). Furthermore, because it is based on the lightest metal that can commonly attain the +III oxidation state, MIL-100(Al) is more promising for gravimetric gas sorption applications owing to its lower density.

Experimental Section

INSTRUMENTS

Powder diffraction data were collected on a STOE STADI P Combi diffractometer using either Mo Kα radiation (50 kV, 40 mA) or Cu Kα radiation (40 kV, 40 mA) (graphite primary monochromator). The diffracted beam was recorded on a DECTRIS MYTHEN 1K strip detector. The samples were loaded in 0.7 mm diameter capillaries, aligned to the geometric center of the diffractometer, and measured in transmission, with independent 2-theta movement.

Published in : Inorganic Chemistry (2021), vol. 60, n°21, pp. 16666-16677
DOI: 10.1021/acs.inorgchem.1c02568
Status : Postprint (Author's version)

Infrared spectra were recorded in the 4000–370 cm^{-1} range on a Bruker Alpha spectrometer equipped with a Platinum ATR module (diamond crystal) housed in an argon-filled glovebox.

Thermogravimetric analysis (TGA) measurements of the MOFs were performed on a Mettler Toledo TGA/DSC^{3+} system equipped with a sample robot. The air flow was 100 mL/min. An initial isotherm at 27 °C was applied for 15 min before heating the sample up to 900 °C at a rate of 10 K/min. TGA-MS was done by coupling a ThermoStar GSD 301 T mass spectrometer to the outlet of the TGA oven.

Nitrogen sorption isotherms were measured at 77 K using Micromeritics ASAP2020 equipment. All samples were activated at 200 or 150 °C (depending on the sample) under dynamic vacuum for 10 h prior to analysis.

Transmission electron microscopy (TEM) images were obtained using an LEO 922 Omega Energy Filter Transmission Electron Microscope operating at 120 kV. The samples were suspended in ethanol, and a drop of the suspension was deposited on a holey carbon film supported on a copper grid (Holey Carbon Film 300 Mesh Cu, Electron Microscopy Sciences), which was dried overnight at room temperature before introduction in the microscope.

Solution-state ^{1}H NMR spectra were recorded at room temperature (296 K) on a Bruker Avance II 300 spectrometer operating at 300.1 MHz. Experiments were run under the TopSpin program (3.2 version, Bruker) using a BBFO {^{1}H, X} probe head equipped with a *z*-gradient coil. ^{1}H chemical shifts are reported in parts per million (ppm) and referenced to the residual signal of DMSO-d_5 (δ 2.50 ppm). The samples were prepared by adding an appropriate amount of solid to a glass test tube equipped with a ground glass joint. For activation, a glass stopcock, connected to a vacuum supply (via a Schlenk line), was adapted on the test tube and heating was applied using an oil bath. About 0.5 mL of D_2SO_4 was then added to the sample using a glass pipette, followed by an appropriate amount (enough to obtain a clear solution after heating) of DMSO-d_6. The test tube was then sealed with a glass stopper, and the mixture was heated using a heat gun until a clear solution was obtained (in the case of difficult solubilization, some DMSO-d_6 was added and the mixture was heated again to obtain a clear solution). The solution was then cooled and transferred into a 5 mm thin-walled precision NMR sample tube for analysis. Note: The added volume of DMSO-d_6 is variable depending on the sample to dissolve. The total quantity needed to achieve complete dissolution is dependent on the nature of the sample (portions of ~0.5 mL were added until a clear solution was obtained). This results in variable D_2SO_4/DMSO ratios for each analyzed sample and in slight shifts of peak positions in the ^{1}H NMR spectra but does not affect the quantification of the EN/H_3BTC ratio.

Published in : Inorganic Chemistry (2021), vol. 60, n°21, pp. 16666-16677
DOI: 10.1021/acs.inorgchem.1c02568
Status : Postprint (Author's version)

Solid-state ^{13}C and ^{15}N cross-polarization (CP) magic-angle spinning (MAS) NMR spectra were acquired at room temperature on a Bruker Avance-500 NMR spectrometer operating at 11.7 T (125.8 MHz for ^{13}C and 50.6 MHz for ^{15}N) and equipped with a 4 mm CP-MAS Bruker probe. ^{13}C CP-MAS spectra were recorded using a contact time of 2 ms, a spinning rate of 10 kHz, a relaxation delay of 5 s, and 1000 scans. The ^{15}N CP-MAS spectrum was recorded using a contact time of 2 ms, a spinning rate of 8 kHz, a relaxation delay of 10 s, and 92 000 scans. The processing comprised exponential multiplication of the free induction decay with a line broadening factor of 10 Hz, zero filling prior to Fourier transform, phase, and baseline corrections. Chemical shift scales were referenced externally to solid adamantane (^{13}C: 38.68 ppm) and ammonium chloride (^{15}N: 39.3 ppm). (23,24) Solid-state ^{27}Al MAS NMR spectra were acquired at room temperature on a 400 MHz Varian VNMRS spectrometer operating at 9.4 T (104.2 MHz for ^{27}Al) and equipped with a 4 mm Chemagnetics T3 probe. MAS spectra were recorded using a spinning rate of 8 kHz. Processing comprised manual baseline correction. Chemical shifts were referenced externally to aluminum nitrate in H_2O (^{27}Al: 0.0 ppm). Note: The MIL-100(Al) sample that was used for solid-state NMR investigations was first activated and then rehydrated by prolonged exposure to air for several days.

Solid-state UV–vis measurements of bromothymol blue impregnated samples were performed on a Shimadzu UV-3600 Plus UV–Vis–NIR spectrometer equipped with a Harrick single-beam Praying Mantis Diffuse Reflectance collection system. A Spectralon Diffuse Reflectance Standard was used to measure the background spectra.

Solution-state UV–vis measurements of the ninhydrin tests were collected on a 1700 UV/visible spectrophotometer from Shimadzu.

Volumetric carbon dioxide sorption experiments were performed on an IMI-HTP Sievert's apparatus from Hiden Isochema. For the experiments, about 100 mg of sample was used and activated under vacuum at 100 or 200 °C before sorption experiments. The excess uptake values were converted to mmol/g of dry sample based on the sample's weight after activation.

Gravimetric cyclic sorption experiments were performed on a Mettler Toledo TGA/DSC^{3+} system. For each experiment, the sample was activated *in situ* in the thermogravimetric analyzer by heating (10 K/min) to 100 °C (2 h isotherm) and cooling back to 25 °C (10 K/min) and maintaining this temperature for 90 min, all of these operations were performed under helium (100 mL/min). The adsorption/desorption cycles were realized by switching gas fluxes every 60 min from helium (100 mL/min) to carbon dioxide (100 mL/min) and vice-versa at a constant temperature of 25 °C.

Elemental analyses (ICP and CHN) were performed by Medac Ltd. (U.K.).

Published in : Inorganic Chemistry (2021), vol. 60, n°21, pp. 16666-16677
DOI: 10.1021/acs.inorgchem.1c02568
Status : Postprint (Author's version)

Gravimetric CO_2 low-pressure sorption isotherms were performed using a Netzsch STA 449 F3 TGA instrument equipped with a stainless steel oven hosted in an argon-filled glovebox. The sample was subjected to a constant gas flux of 100 mL/min of an Ar/CO_2 mixture with an increasing proportion of CO_2 every 30 min (0, 5, 10, 15, 20, 25, 30, 40, 50, 60, 70, and 80%) under a constant temperature of 27 °C. The adsorption was followed by 90 min desorption under a flux of 100 mL/min of argon. The mass increase at equilibrium after 30 min of exposure to each gas mixture of a given composition was plotted against the partial pressure of CO_2 to obtain the corresponding adsorption isotherm. The samples were degassed at 100 °C under vacuum *ex situ* before the experiments and transferred to the glovebox without contacting air.

CHEMICALS

Trimesic acid (98%), heptane (99%), thiophosgene (85%), iodomethane (99%, stabilized), dry ether (99.5%, extra dry), triethylamine (99%), and toluene (99.85%, Extra Dry, AcroSeal) were purchased from Acros Organics. Denatured ethanol (Technisolv, 99%), dimethylformamide (HiPerSolv, CHROMANORM), methanol (HiPerSolv, CHROMANORM), dichloromethane (DCM, HiPerSolv, CHROMANORM), pentane (HiPerSolv, CHROMANORM), hexane (HiPerSolv, CHROMANORM), sodium hydroxide pellets, HCl 37% (AnalaR, NORMAPUR), and ninhydrin (AnalaR, NORMAPUR ACS, Reag. Ph. Eur., for analysis) were purchased from VWR Chemicals. D_2SO_4 and DMSO-d_6 were purchased from Euriso-top. Ethylenediamine (>99.5%), boron trifluoride diethyl etherate, aluminum chloride (98%), and hexylamine (99%) were purchased from Merck. Bromothymol blue was purchased from Alfa Aesar. All chemicals were used as received.

SYNTHETIC PROCEDURES

Gram Scale Synthesis of MIL-100(Al)

Caution! This synthesis employs large amounts of chemicals; therefore, precautions must be taken. This is especially the case for the dissolution of aluminum chloride in water, which is extremely exothermic and may release hydrogen chloride. Therefore, this dissolution must be performed under an efficient fume hood using good quality borosilicate, thick-walled glassware. Water must be poured as quickly as possible on $AlCl_3$ to avoid overheating. This step causes impressive and excessive fuming. *Preparation of solution A*: A total of 31.5 g of trimesic acid was dissolved in 3 L of denatured ethanol in a 4 L Erlenmeyer flask. The flask was shaken until all of the acid was completely dissolved. Stepwise addition of the acid and sonication are recommended for avoiding the formation of aggregates and speeding up the process. Once a clear solution was obtained, 3.15 mL

Published in : Inorganic Chemistry (2021), vol. 60, n°21, pp. 16666-16677
DOI: 10.1021/acs.inorgchem.1c02568
Status : Postprint (Author's version)

of concentrated hydrochloric acid was added and the mixture was homogenized by shaking. *Preparation of solution B*: A total of 17.25 g of $AlCl_3$ was added in a dry 4 L Erlenmeyer flask. Then, 3 L of demineralized water was added through a large glass funnel, and the first 1000 mL were added as fast as possible (Exothermic reaction!). The mixture was homogenized, followed by the addition of 35.0 mL of DMF. The flask was shaken to obtain a homogeneous mixture. *Preparation of the MOF*: Solutions A and B were mixed together in a 10 L polyethylene can. The can was closed with a screw cap and thoroughly shaken to obtain a homogeneous mixture. The mixture was then poured into glass bottles (10 bottles of 500 mL capacity, each containing 400 mL of the reaction mixture, and 1 bottle of 2.5 L capacity containing 2000 mL of the mixture). All of the bottles were placed into an oven at 83 °C for 6 days. The white precipitate was centrifuged at 6000 rpm and washed with water (3 times) and ethanol (3 times). The powder was then suspended in a minimum amount of ethanol, and the suspension was evaporated under reduced pressure at 70 °C using a rotary evaporator.

Small-Scale Syntheses of Al-BTC MOFs

Solutions A and B were prepared as described above (in smaller volumes). Then, 200 mL of each solution were mixed together in 500 mL screw-capped glass bottles. The bottles were sealed and placed in an oven at 80 °C for a given amount of time (4, 5, 6, 8, 11, or 15 days). The white precipitate was centrifuged at 4000 rpm and washed with water (3 times) and ethanol (3 times). The powder was then suspended in a minimum amount of ethanol, and the liquid was evaporated under reduced pressure at 70 °C using a rotary evaporator. Note that the rotation speed during the centrifugation is lower than for the large-scale synthesis (the speed for the large-scale synthesis was increased to recover more material). This has two consequences on the obtained product: (1) more material is recovered when using higher speed (the supernatants are not clear solutions but have an aspect similar to milk) and (2) the size distribution of the particles changes when higher speeds are used; this can be seen by broadening of the powder X-ray diffraction (PXRD) peaks and on the Barrett–Joyner–Halenda (BJH) pore size distribution of the materials. The presence of very small (nano)-particles is in agreement with the aspect of the supernatants.

Synthesis of the Bimetallic MIL-100(Fe,Al) MOF

The synthesis was adapted from a procedure described previously by us, (25) using an 8/2 starting molar ratio of Fe/Al and setting the reaction time to 10 h instead of 16 h, allowing the incorporation of a higher amount of Al compared to Fe (leading to an Fe/Al ratio of 2/1 in the final material).

Functionalization with Ethylenediamine

Published in : Inorganic Chemistry (2021), vol. 60, n°21, pp. 16666-16677
DOI: 10.1021/acs.inorgchem.1c02568
Status : Postprint (Author's version)

The following procedure was adapted from an earlier report describing the synthesis of EN@MIL-100(Cr). (17) A total of 1.2 g of as-synthesized MIL-100 was introduced into a 250 mL three-neck flask equipped with a condenser, a rubber septum, and a glass stopcock. The MOF was heated at 200 °C under vacuum (using the glass stopcock connected to a Schlenk line) overnight for activation. The flask was subsequently allowed to cool down under vacuum, and the stopcock was closed. Then, 120 mL of anhydrous toluene was added using a syringe. Once the toluene was added, the flask was backfilled with argon. Note: adding the toluene when the flask is under vacuum allows wetting the MOF powder so that it does not fly up in the flask when the volume is backfilled with argon. The suspension was stirred to disperse the MOF, and 0.10 mL of ethylenediamine was added by a syringe. The stopcock was closed again, and an argon-filled balloon was added at the top of the condenser. The mixture was then refluxed for 12 h. After cooling down the flask, the mixture was centrifuged and the toluene supernatant was discarded. The solid was then washed 3 times with *n*-hexane and 2 times with *n*-pentane. The obtained solid was then dried, while still being in the (open) centrifugation tubes, in an oven under air at 45 °C for 3 h to afford a powder of the functionalized MOF (white powder for EN@MIL-100(Al); brown powders for EN@MIL-100(Fe) and EN@MIL-100(Fe,Al)).

Synthesis of the 8-Thiomethyl-BODIPY Fluorescent Dye

The BODIPY dye was synthesized according to a reported three-step procedure, (26) with small modifications. In brief, a solution of freshly distilled pyrrole (4.2 mL in 90 mL of dry ether) was added dropwise to a thiophosgene solution (2.3 mL in 80 mL of dry toluene) in an ice bath (0 °C) under argon using a syringe. After complete addition, the solution was stirred for 30 min. The reaction was then quenched by the addition of 100 mL of a 10 mol % NaOH solution in water/methanol (10:90 v/v), followed by 1 h of stirring at room temperature. The solvent was then removed in vacuo, and the resulting crude product was purified on a short silica pad using a heptane/DCM (1:3 v/v) mixture containing 1% triethylamine. Only the bright orange fraction was collected, and the solvents were evaporated in vacuo, yielding red crystals of high purity of bis-(1*H*-pyrrol-2-yl)-methanethione. ^{1}H NMR ($CDCl_3$, 300 MHz, 293 K): δ 7.80 (2H, m), 7.42 (2H, m), 6.53–6.54 (2H, m), 2.91 (3H, s). A total of 0.45 g of the obtained product was subsequently dissolved in 7.4 mL of DCM under an argon atmosphere, followed by the addition of 2.9 mL of methyl iodide. The mixture was stirred for 26 h at room temperature, and the solvent was evaporated in vacuo. The obtained crude 2-[methylsulfanyl-(1*H*-pyrrol-2-yl)-methylene]-2*H*-pyrrolium iodide was used for the last step of the synthesis without further purification or analysis. Then, 0.88 g of the obtained product was dissolved in 19 mL of DCM

Published in : Inorganic Chemistry (2021), vol. 60, n°21, pp. 16666-16677
DOI: 10.1021/acs.inorgchem.1c02568
Status : Postprint (Author's version)

under an argon atmosphere, followed by the addition of 2 mL of triethylamine and subsequent stirring at room temperature for 40 min. Then, 1.63 mL of $BF_3{\cdot}Et_2O$ was added and the mixture was stirred further for 24 h. Solvents were removed in vacuo, and the obtained crude product was dissolved in some DCM. The product was purified by chromatography on silica by subsequently using heptane/DCM/triethylamine mixtures with various solvent ratios (100:10:1.1 → 100:100:2 → 50:100:1.5). A second purification, consisting of washing in water and extraction in toluene, allowed obtaining high purity 8-(thiomethyl)4,4-difluoro-4-bora-3*a*,4*a*-diaza-s-indacene (BODIPY).

Postfunctionalization with BODIPY Dye

A total of 50 mg of as-synthesized (nonactivated) MOF sample was soaked in a 15 mL of solution of the BODIPY probe in dichloromethane (1 mg in 100 mL) and stirred for 10 min before being filtered and washed with dichloromethane on a PTFE filtration membrane (pore size 0.45 μm). The BODIPY functionalized samples were finally air-dried.

NINHYDRIN AND BROMOTHYMOL BLUE TESTS

Ninhydrin Test

First, a solution of 5×10^{-3} M of ninhydrin in ethanol was prepared. Then, a calibration plot was determined with hexylamine as a standard primary amine. A specific amount of hexylamine solution (between 5×10^{-5} and 8.3×10^{-4} M) was mixed with ninhydrin for 2 h at 65 °C, then cooled for 15 min at room temperature. The primary amine peak appears at 580 nm (blue coloration). Suspensions of 0.5 g/L of activated MOFs (recovered after Brunauer–Emmett–Teller (BET) analysis) were prepared in ethanol and dispersed for 5 min under ultrasonic treatment. Then, 2 mL of these suspensions were mixed with 1 mL of ninhydrin solution for 2 h at 65 °C and cooled at room temperature for 15 min. The samples were centrifuged at 15 000 rpm for 30 min. Then, the UV–vis spectra of the supernatants were measured with the spectrophotometer and the concentration of primary amine was estimated thanks to the absorbance measured at 580 nm and the calibration plot.

Acidity Determination by Adsorption of Bromothymol Blue

A transparent solution of bromothymol blue in toluene was prepared (50 mg in 100 mL), and about 10 mL of this solution was added to 50–100 mg of the solid to be analyzed (a nonactivated MOF or a reference sample) in a test tube. The solution was stirred with a glass rod until the sample was colored (about 1 min). Then, the solid was decanted, toluene was removed using a pipette, and the sample was washed twice with *n*-hexane and once with *n*-pentane, followed by drying in a vacuum

Published in : Inorganic Chemistry (2021), vol. 60, n°21, pp. 16666-16677
DOI: 10.1021/acs.inorgchem.1c02568
Status : Postprint (Author's version)

oven at 60 °C for about 30 min. The diffuse reflectance spectra of the obtained samples were then measured.

Results and Discussion

COLLAPSE OF MIL-100(FE) UPON CONTACT WITH ETHYLENEDIAMINE

Our first attempt concerned the functionalization with ethylenediamine of MIL-100(Fe), which was obtained using a previously described method. (25) To do so, the synthesized MOF was first activated by heating under vacuum at 200 °C to remove the physisorbed and coordinated solvent molecules and was then refluxed under argon in toluene in the presence of EN. However, the powder X-ray diffraction (PXRD) pattern of MIL-100(Fe) after this treatment revealed that the compound had completely lost its crystallinity, becoming amorphous (see the Supporting Information, Figure S1). Significant changes were also observed in the Fourier transform infrared (FTIR) spectrum of MIL-100(Fe) after the reaction with EN (see the Supporting Information, Figure S2). This shows that MIL-100(Fe) cannot be functionalized with ethylenediamine without collapsing using toluene as a solvent, unlike the more robust MIL-100(Cr), which possesses a well-known framework stability thanks to the kinetic inertness of Cr^{3+} complexes. (16,17) Coordinating solvents that can compete with ethylenediamine, like ethanol, have, however, been reported to allow the functionalization of this MOF with EN (27) or other amines (28) with at least partial retention of the crystal structure. The lower stability of MIL-100(Fe) compared to its Cr-analogue can be explained by the fact that it, and Fe-complexes in general, possesses kinetic lability of the linkers bound to Fe and because Fe^{3+} can be reduced to Fe^{2+}, which forms weaker bonds with carboxylate linkers.

OPTIMIZED SYNTHESIS OF MIL-100(AL)

Regarding MIL-100(Al), most reports on the synthesis of this particular MOF use hydro- or solvothermal processes involving high reaction temperatures requiring autoclaves. (29−31) We thus attempted an approach using a lower temperature, set at 80 °C. We obtained the Al-based MOF by mixing an ethanol solution containing trimesic acid and some HCl with an aqueous solution of $AlCl_3$ containing some DMF (see the Experimental Section for details). The obtained mixture was incubated in closed screw-capped glass bottles in an oven at 80 °C, and the resulting white precipitates were washed with water and ethanol and collected by centrifugation followed by drying under vacuum.

Nitrogen sorption experiments were performed on MOF samples obtained after different incubation times to evaluate their specific surface area by the Brunauer–Emmett–Teller (BET) and Langmuir

Published in : Inorganic Chemistry (2021), vol. 60, n°21, pp. 16666-16677
DOI: 10.1021/acs.inorgchem.1c02568
Status : Postprint (Author's version)

methods (Figure 1A) as well as their Barrett–Joyner–Halenda (BJH) pore size distribution (Figure 1B). From the obtained results, it is clear that a maximum surface area is obtained after 6 days of reaction (S_{BET} = 1937 m^2/g); longer reaction times leading to a continuous decrease of surface areas. Overall, all of the obtained MOF samples have quite large surface areas compared with the ones of other reported syntheses (see Table S3): between 1479 and 1937 m^2/g (BET) or 2019 and 2667 m^2/g (Langmuir) (Figure 1A).

Figure 1

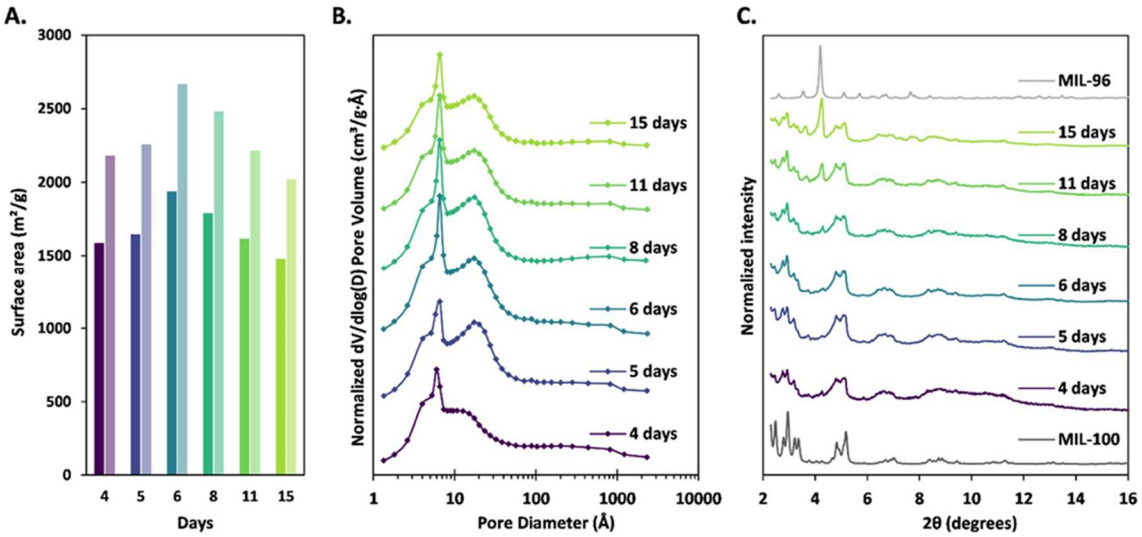

Figure 1. (A) Evolution of the Brunauer–Emmett–Teller (dark colors) and Langmuir (light colors) surface areas of Al-BTC MOF samples obtained after different reaction times. Both BET and Langmuir values are given, as these are the most commonly reported textural data in the literature for MOFs. (B) Evolution of the Barrett–Joyner–Halenda pore size distribution of Al-BTC MOF samples obtained after different reaction times. (C) PXRD patterns of Al-BTC MOF samples obtained after different reaction times, along with simulated patterns of MIL-100 and MIL-96 for comparison (wavelength: 1.5406 Å).

To determine why the evolution of the surface area went through a maximum, powder X-ray diffraction (PXRD) patterns of all samples were measured after activation by heating under vacuum at 200 °C for 10 h (Figure 1C). The MOFs obtained after 4, 5, and 6 days of reaction time show the presence of a pure MIL-100 phase, whereas the samples isolated after longer reaction times also contain MIL-96 as a secondary phase. Therefore, the samples obtained during this optimization step were named "Al-BTC" as they are not all phase pure. MIL-96 is another Al-BTC MOF having a lower surface area than MIL-100, (32,33) thus explaining why it decreases after 6 days of reaction. The formation of MIL-96 upon longer reaction times can be explained by its better thermodynamic stability. (30) The presence of unreacted trimesic acid in the pores of the compounds, which is commonly encountered when other preparation methods are used, can be excluded according to

Published in : Inorganic Chemistry (2021), vol. 60, n°21, pp. 16666-16677
DOI: 10.1021/acs.inorgchem.1c02568
Status : Postprint (Author's version)

the FTIR spectra of the different samples (Figures 2A and S3), as the characteristic bands of C═O (1720 cm^{-1}) and C–O (1349 and 1273 cm^{-1}) stretching of free H_3BTC are not present. (34) The increase of the surface area between 4 to 6 days of reaction is presumably due to the slow formation and crystallization of MIL-100, leading to the highest quality MIL-100(Al) sample after 6 days.

Figure 2

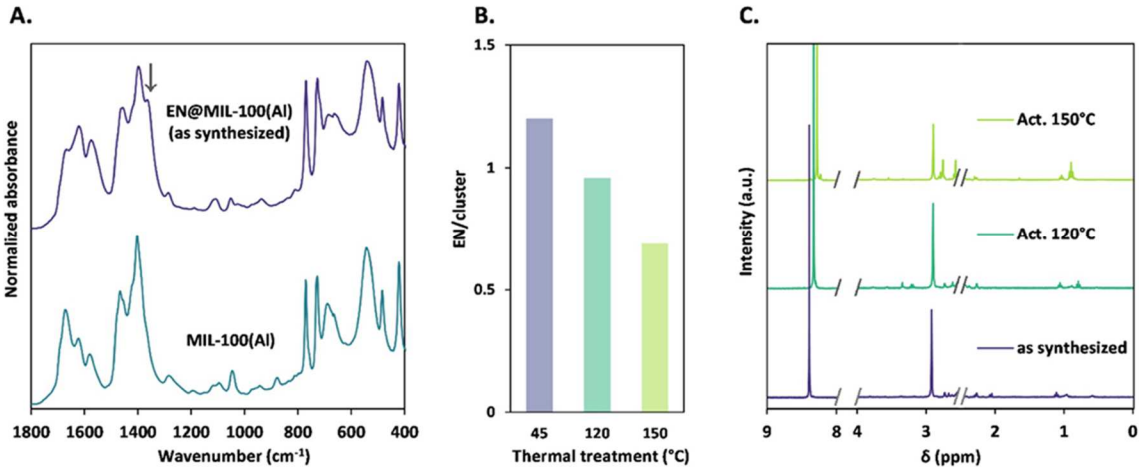

Figure 2. (A) FTIR spectra of as-synthesized MIL-100(Al) and EN@MIL-100(Al) MOFs, the arrow indicates the peak corresponding to the C–N stretch of ethylenediamine. (B) EN/cluster ratios calculated from integration of the linker and ethylenediamine peaks in ^{1}H NMR spectra of digested EN@MIL-100(Al) samples treated at different temperatures (45 °C = as-synthesized sample, 120 and 150 °C were heated under vacuum). (C) Solution-state ^{1}H NMR spectra of the as-synthesized and activated EN@MIL-100(Al) digested samples.

To our delight, the BJH pore size distribution plots show the presence of not only micropores in the materials but also small mesopores with a diameter of around 20 Å (Figure 1B). The presence of such mesopores would not be expected based on the crystal structures of MIL-100 or MIL-96, which are both microporous and should give rise to a type I isotherm. Furthermore, the nitrogen sorption isotherms displayed a hysteresis (see the Supporting Information, Figures S4 and S5), which is not what would be expected for microporous compounds. The mesoporous nature of those cavities is furthermore indicated by the shape of the hysteresis, intermediate of the H2(b) and H5 types according to IUPAC classification, which is both typical of the presence of mesopores in the material. (35) This led to the conclusion that the obtained materials possess hierarchized porosity. This is a useful textural feature because large pores are of interest to keep large surface areas upon functionalization of MOFs, and hierarchized solids allow faster diffusion of guest molecules through the porous framework. (36) The analysis of the BJH plots shows that there is also an optimum of the pore size distribution after 6 days of reaction. Moreover, the presence of a second hysteresis in the

Published in : Inorganic Chemistry (2021), vol. 60, n°21, pp. 16666-16677
DOI: 10.1021/acs.inorgchem.1c02568
Status : Postprint (Author's version)

adsorption isotherms at partial pressures close to unity with a characteristic shape of a H3 type according to IUPAC is typical of nonrigid aggregates of plate-like particles. Transmission electron microscopy (TEM) imaging shows that the obtained solid is indeed composed of such aggregates (Figure S10).

Given the interesting textural properties of the obtained MIL-100(Al) MOF, we decided to investigate the possibility to scale-up the synthesis as the yield was quite low. For this purpose, several liters of precursor solution were prepared (see the Experimental Section for the detailed procedure) and the MOF was successfully obtained on a gram scale by applying the optimized reaction conditions. The scaled-up sample was characterized and showed good phase purity (see the Supporting Information) and was thus used for further experiments, and named MIL-100(Al), in contrast with the samples resulting from the small-scale synthesis optimization. However, it should be noted that higher centrifugation speeds were used for recovering this sample, which led to the collection of smaller particles, as supported by TEM imaging (Figure S10). Therefore, a large amount of interparticle voids has also been formed in this sample. This is supported by a much more significant H3 type hysteresis at partial pressures close to unity on the nitrogen sorption isotherms (Figure S6) and the presence of porosity in the range of macropores on the BJH plots (Figure S7). However, the surface area of the obtained MOF samples was comparable to the sample from the small-scale synthesis (Figure S8) and the ratio between the *t*-plot calculated surface areas of micropores and the external surface area remained constant (Figure S9), mainly because interparticle voids develop small surface areas.

SUCCESSFUL FUNCTIONALIZATION OF AL-CONTAINING MIL-100 WITH EN

To perform functionalization with EN, the sample was activated under vacuum at 200 °C and then reacted with ethylenediamine in refluxing anhydrous toluene. The sample was then isolated by centrifugation, washed with hexane and pentane, and dried in air at 45 °C to yield EN@MIL-100(Al). The obtained powder was characterized by PXRD (Supporting Information, Figure S1), showing that the structure did not undergo collapse during the functionalization procedure by opposition to MIL-100(Fe). Aluminum-based MIL-100, unlike its Fe analogue, is thus resistant enough to retain its structure upon reaction with EN. This shows that the choice of the metal composing the MOF rather than the MOF's structure is of critical importance for achieving efficient grafting of EN. Interestingly, a bimetallic MIL-100(Fe,Al) MOF (the preparation and detailed characterization of the bimetallic nature is described elsewhere), (25) characterized by a Fe/Al ratio of about 2/1 (determined by inductively coupled-plasma optical-emission spectroscopy (ICP-OES), see Table S4), resists the

Published in : Inorganic Chemistry (2021), vol. 60, n°21, pp. 16666-16677
DOI: 10.1021/acs.inorgchem.1c02568
Status : Postprint (Author's version)

same treatment with ethylenediamine, showing that Al stabilizes the structure, even when present in rather low concentrations in the MOF (see the Supporting Information for more details, Figures S1 and S2). This observation is likely related to the higher strength of the Al–O bonds compared to Fe–O. Thermogravimetric analysis (TGA) (Supporting Information, Figure S11) of EN@MIL-100(Al) showed a decomposition temperature very close to the one of pristine MIL-100(Al) (∼430 °C). A rather continuous weight loss, attributed to guest species (*i.e.*, EN and solvent molecules), is taking place before decomposition.

The nitrogen sorption isotherms of EN@MIL-100(Al) after activation at 150 °C (Supporting Information, Figure S12B.) revealed a BET surface area decrease from 1861 m^2/g for pristine MIL-100(Al) to 657 m^2/g upon functionalization (−64.7%), owing to the EN molecules partly occupying the volume of the pores. For the bimetallic MOF, a surface area decrease was also observed (Supporting Information, Figure S12C) from 1029 to 839 m^2/g after functionalization (−18.5%). For MIL-100(Fe), the nitrogen sorption isotherms (Supporting Information, Figure S12A) confirmed that the large surface-area MOF (2048 m^2/g) completely collapsed, leading to a nonporous (3.98 m^2/g) compound after contact with EN in toluene.

The effectiveness of the grafting on MIL-100(Al) was evidenced by the FTIR spectrum (Figure 2A), presenting characteristic absorption bands expected for ethylenediamine grafting, especially visible at 1370 cm^{-1}. The presence of EN in the MOF was further confirmed by solution-state ^1H NMR experiments on the digested MOF (details about ^1H NMR analysis and reference sample measurements can be found in the Experimental Section and Supporting Information, Figure S14). The spectrum of activated MIL-100(Al) presents a singlet at 8.14 ppm, corresponding to the aromatic signals of the trimesate linker, whereas the spectrum of digested EN@MIL-100(Al) shows the same peak (downshifted to 8.28 ppm, due to differences in D_2SO_4 concentration of the solution) and a supplementary singlet at 2.90 ppm, unambiguously demonstrating the presence of ethylenediamine. The ratio of the integrals of the peaks of the aromatic protons of the linker and the protons of EN allowed us to determine the number of EN molecules per cluster (Figure 2B,C; see also the Supporting Information for details on calculations based on the MOF's structure). The as-synthesized sample achieved 1.2 EN/cluster on average. A portion of the sample was heated under vacuum to remove physisorbed EN and was subsequently digested for ^1H NMR analysis. As expected, the amount of EN decreased somewhat when the sample was heated to 120 °C, to reach a 0.96 EN/cluster on average. Heating to 150 °C, however, led to decomposition of part of the EN present in the pores (see the Supporting Information, Figure S14, for detailed NMR spectra). Our results show

Published in : Inorganic Chemistry (2021), vol. 60, n°21, pp. 16666-16677
DOI: 10.1021/acs.inorgchem.1c02568
Status : Postprint (Author's version)

that about one out of three Al sites is occupied by EN, which is in agreement with previous reports stating that only one Al per cluster can be coordinatively unsaturated by activation under vacuum, (34) and thus accept an EN molecule.

The FTIR spectra of the bimetallic MIL-100(Fe,Al) before and after functionalization with EN, unfortunately, do not display evident differences demonstrating the presence of ethylenediamine inside the MOF (Figure S2). Also, given the paramagnetic nature of the iron present in the MOF, characterization by digestion and ^{1}H NMR analysis is not straightforward, as this would require the elimination of iron species prior to analysis. Therefore, the determination of the presence of EN in the bimetallic materials was performed by combining the results from ICP-OES and CHN elemental analyses (see Table S4), as no N containing solvents were used throughout the synthesis procedures, enabling us to hypothesize that all of the nitrogen contents originate from the presence of ethylenediamine. From these determinations, the N/metal content could be determined for the as-synthesized samples, as well as after degassing under vacuum at 100 °C. The EN/metal ratio is equal to 1.9 for the as-synthesized material and to 1.8 after heating at 100 °C, indicating that about two out of three metal centers are coordinated to EN on average. However, it was not possible from these analyses to determine whether coordination occurs on either Fe or Al or on both metals. ICP analysis further showed that the Fe/Al ratio remained constant, which is equal to 2/1 before and after functionalization, showing that no metal leaching occurred during the reaction with EN. It is noteworthy that although, after functionalization, the EN content of the bimetallic MOF is twice as high as for the monometallic one, the percentage of decrease in the surface area for MIL-100(Al) is about 3.5 times higher than for MIL-100(Fe,Al). Such a huge difference cannot simply be explained by the difference of molar mass between both MOFs (586 g/mol for $Fe_2AlO(OH)BTC_2$ and 546 g/mol for $Al_3O(OH)(H_2O)BTC_2$). The explanation for this observation most likely lies in the fact that in the bimetallic MOF, the ethylenediamine molecules occupy the mesoporous voids of the material, leaving the large surface area developed by micropores mostly unaffected. This is supported by the decrease of the size of the hysteresis loop in the partial pressure range between 0.5 and 0.7 on the nitrogen sorption isotherm after functionalization (Figure S12C), as well as by the change of the pore size distribution (Figure S13B). In contrast, the pore size distribution of MIL-100(Al) does not change significantly after functionalization (Figure S13A), indicating that in this MOF, the functionalization occurs homogeneously throughout the framework.

Thermogravimetric analyses were performed to probe the thermal stability of the MOFs before and after functionalization, and coupling to MS was used to determine the temperature at which EN

Published in : Inorganic Chemistry (2021), vol. 60, n°21, pp. 16666-16677
DOI: 10.1021/acs.inorgchem.1c02568
Status : Postprint (Author's version)

leaves the framework of the functionalized materials (see Figure S11 and the corresponding note in the Supporting Information for details). Concerning MIL-100(Fe), a completely different decomposition temperature was observed for the pristine MOF (~320 °C) and the product obtained after reaction with ethylenediamine (~300 °C). Such a difference is expected as the nature of both samples is different given the collapse of the MOF upon contact with EN. For the bimetallic and monometallic Al-based samples, the decomposition temperature remained unchanged upon functionalization, the bimetallic compounds having a decomposition temperature very close to that of monometallic MIL-100(Fe) (~320 °C), whereas the Al-based MOFs have a higher decomposition temperature close to 430 °C. Based on analysis of MS fragments with m/z values of 30, 42, and 43 (see the Supporting Information for detailed explanation), it seems that EN leaves the framework of EN@MIL-100(Al) around 290 °C, well below the framework's decomposition temperature. For EN@MIL-100(Fe,Al), it seems that EN remains in the framework until decomposition (~320 °C). Although the difference in the observed temperatures at which EN leaves the MOFs could indicate stronger binding to Fe than to Al, these deductions are only based on a few fragments in the mass spectrum of ethylenediamine and must not be overinterpreted. Indeed, degradation of EN in the framework can occur well below the temperatures indicated by TGA-MS, as shown by the solution NMR experiments on digested EN@MIL-100(Al) (*vide supra*).

Given that the monometallic Al-containing samples contain only nonparamagnetic nuclei and that, furthermore, all of these nuclei possess at least one NMR-active isotope, the grafting of EN could also be nicely evidenced by solid-state NMR CP-MAS experiments. ^{13}C spectra of MIL-100(Al) show signals around 170 and 130 ppm for the carboxylate and aromatic carbons, respectively. (34) Upon EN addition, a separated signal around 38 ppm is clearly observed due to the aliphatic chain of the added ligand (Figure 3A). Besides that, the ^{15}N solid-state NMR spectrum (Figure 3B) shows the presence of two signals of comparable intensities at 25 and 31 ppm, upshifted with respect to liquid (neat) EN (17.8 ppm, not shown). These results indicate that the two nitrogen atoms experience a similar environment, in agreement with the results reported in the literature (37) and the EN grafting model we propose (see the inset of Figure 3B) with one Al-coordinated nitrogen atom and one free amine group. Signals of the ^{27}Al spectra of both pristine and functionalized MOFs (Figure S15) present a chemical shift around 0 ppm, similar to the previously reported spectra of hydrated MIL-100(Al), (34) confirming that the metallic centers are six-coordinated. Furthermore, after functionalization with EN, the resulting signal possesses a more important downfield contribution, which can be

Published in : Inorganic Chemistry (2021), vol. 60, n°21, pp. 16666-16677
DOI: 10.1021/acs.inorgchem.1c02568
Status : Postprint (Author's version)

explained by an increased p character of the Al–N bond of the metal center with the amine compared to the Al–O bonds with the oxo-, hydroxo-, and carboxylate ligands. (38,39)

Figure 3

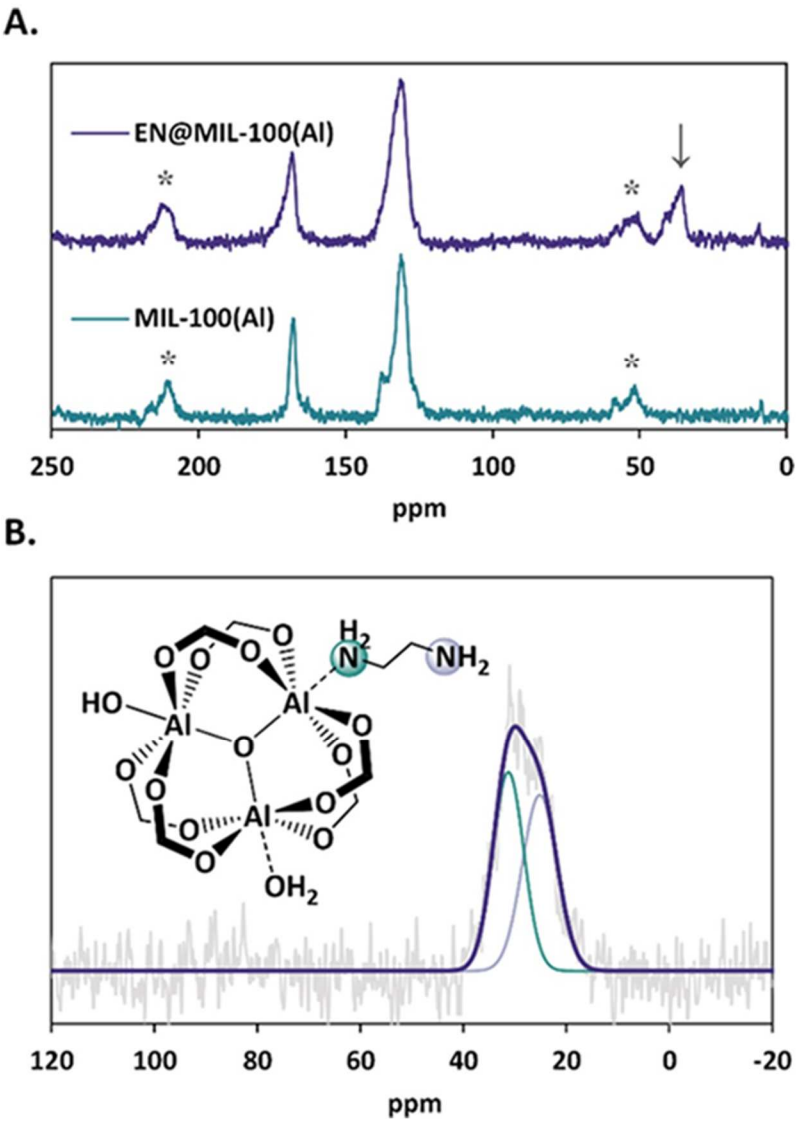

Figure 3. (A) ^{13}C CP-MAS NMR spectra of MIL-100(Al) after activation at 200 °C and of the as-synthesized EN@MIL-100(Al). (B) ^{15}N CP-MAS spectrum of EN@MIL-100(Al) with deconvolution of the signal. The inset is the determined structure of the functionalized cluster units of EN@MIL-100(Al). Asterisks indicate spinning sidebands and the arrow indicates the signal of the aliphatic chain of coordinated EN.

AVAILABILITY OF PENDANT AMINES

The possibility of performing postfunctionalization of the pendant amine sites in the EN@MIL-100(Al) material was investigated through a fast and simple visual test. This was performed using 8-thiomethyl-BODIPY (Figures 4A and S18A). This fluorescent molecule specifically reacts with primary amines, inducing the formation of linked 8-amino-BODIPY (Figure 4B), shifting the emission

Published in : Inorganic Chemistry (2021), vol. 60, n°21, pp. 16666-16677
DOI: 10.1021/acs.inorgchem.1c02568
Status : Postprint (Author's version)

maximum of the free dye from 525 nm (green) to 409–427 nm (blue), allowing us to visually determine whether the reaction occurred. (26,40) To do this, both pristine and ethylenediamine-functionalized MIL-100(Al) were soaked in a dichloromethane solution of 8-thiomethyl-BODIPY and were then recovered by filtration. After this treatment, the pristine MOF showed green fluorescence (Figure 4A), which is typical of the unreacted BODIPY probe, indicating that the molecule was only nonspecifically adsorbed onto the MOF's surface and/or in its pores. In contrast, the EN@MIL-100(Al) sample showed the specific blue fluorescence of the bonded BODIPY fluorophore (Figure 4B), indicating that the postfunctionalization reaction was performed successfully. It should be noted that this methodology was used only to assess the presence of pendant amine sites that are available for postfunctionalization in the material, which could be present either on the MOF's external or internal surface, or both, but not to quantify them, as the BODIPY dye was not used in a stoichiometric amount. Although this test allows to visually evaluate the presence of amines, the fluorescence properties of the resulting solid samples deteriorate with time, likely due to the degradation of the fluorophore, which could be triggered by the acidic and/or basic nature of EN@MIL-100(Al) (*vide infra*), as BODIPY dyes can be decomposed in such media. (41)

Published in : Inorganic Chemistry (2021), vol. 60, n°21, pp. 16666-16677
DOI: 10.1021/acs.inorgchem.1c02568
Status : Postprint (Author's version)

Figure 4

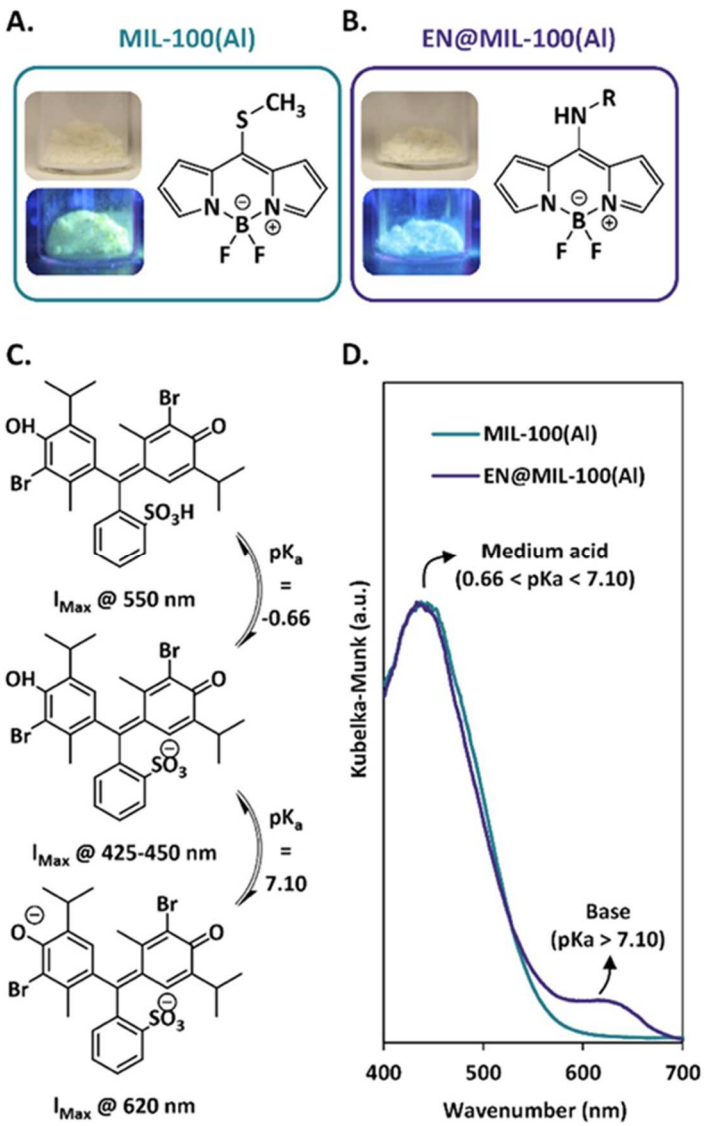

Figure 4. (A, B) Photographs under (upper) visible light and (lower) UV irradiation of (A) MIL-100(Al) and (B) EN@MIL-100(Al) after postfunctionalization with 8-thiomethyl-BODIPY, with structures of the unreacted 8-thiomethyl-BODIPY and the 8-amino-BODIPY grafted upon reaction. (C) Structure of bromothymol blue under different protonation states. (D) Diffuse reflectance UV–vis spectra of BTB impregnated MIL-100(Al) and EN@MIL-100(Al).

Therefore, the degree of availability of the amine functions for medium-sized molecules in the material's bulk was quantified by reaction with ninhydrin (Figure S18B.) in hot ethanol. Ninhydrin specifically reacts to form a blue dye, 2-(1,3-dioxoindan-2-yl)iminoindane-1,3-dione (Figure S18C), that is liberated in solution after its formation. The quantitative analysis of the dye content in the supernatant solution after centrifugal separation of the MOF allows determining the amount of amines that reacted with ninhydrin. (42) The UV–vis spectrum of the supernatant solution after reaction with ninhydrin revealed that reaction with primary amines occurred, as indicated by the

Published in : Inorganic Chemistry (2021), vol. 60, n°21, pp. 16666-16677
DOI: 10.1021/acs.inorgchem.1c02568
Status : Postprint (Author's version)

typical absorption band at 580 nm (Figure S16). To ensure that the obtained results were not due to a reaction with ethylenediamine leached in the hot ethanol solution, a blank test has also been performed. This test consisted of first soaking EN@MIL-100(Al) in boiling ethanol, followed by separation of the supernatant solution by centrifugation. In this case, after performing the ninhydrin test on the supernatant solution, no absorption band appeared at 580 nm (Figure S17), demonstrating that leaching of EN is negligible under the used conditions. Quantitative analysis of the ninhydrin test performed on EN@MIL-100(Al), however, revealed that only 0.6 mmol of $-NH_2$ functions reacted per gram of MOF. This is less than the quantity of free amine functions determined by solution-state ^1H NMR on the digested EN@MIL-100(Al) sample (~1.65 mmol/g or one free $-NH_2$ per Al_3O trimer). This might be explained by the different possible diffusion pathways in MIL-100(Al), either through the larger hexagonal windows with a size of 8.6 Å or through smaller pentagonal windows of 5 Å (Figures S19 and S20). Indeed, although ninhydrin, as well as 2-(1,3-dioxoindan-2-yl)iminoindane-1,3-dione are both small enough to diffuse through the larger windows, diffusion through the smaller ones is impossible, as shown in Figures S18–S21, especially taking into consideration that the pore openings are narrowed by the presence of EN coordinated to the Al_3O clusters. It is possible to calculate the proportion of ethylenediamine molecules that are present in the larger accessible mesopores compared to the amount of total EN. These calculations (see the Supporting Information for details) give a proportion of available ethylenediamine molecules of 41%. This nicely correlates with the 36% of amines detected in EN@MIL-100(Al) by the ninhydrin test (37.5% if considering that only 96% of the clusters are functionalized after thermal activation). This means that the detection efficiency of the amines by the ninhydrin test is about 87–91.5% of the free amines in the large pores. The few percent that are not detected can be ascribed to some adsorption of 2-(1,3-dioxoindan-2-yl)iminoindane-1,3-dione within the framework. These results indicate that it is possible to selectively postfunctionalize part of the EN molecules, localized in the diffusion path of the hexagonal windows, with large molecules while leaving those in the small cages in their pristine state.

BRØNSTED ACIDO-BASICITY OF EN@MIL-100(AL)

It has previously been evidenced that MIL-100(Al) possesses a strong Brønsted acidity due to the presence of water coordinated to the aluminum. (43) We assumed that EN@MIL-100(Al) should possess both Brønsted acidic sites due to the water molecules and Brønsted basic sites due to the presence of $-NH_2$ functions. We decided to investigate this by a method inspired by the one of Hammett, which uses colored pH indicators to probe the strength of acid sites on colorless solids.

Published in : Inorganic Chemistry (2021), vol. 60, n°21, pp. 16666-16677
DOI: 10.1021/acs.inorgchem.1c02568
Status : Postprint (Author's version)

(44) Our method relies on the use of bromothymol blue (BTB), which is fairly soluble in toluene. We used several solids which are known for their strong ($H_3PMo_{12}O_{40}$ and ZSM-5 zeolite) or medium (chromatography silica gel and UiO-66(Zr) MOF) Brønsted acidity, their strong basicity ($NaAlO_2$, Al_2O_3, MgO), as well as mixtures thereof (SiO_2/Al_2O_3 in various ratios) as reference materials (see the Supporting Information, Figure S22). In practice, the solids are immersed in the BTB solution and are repeatedly washed with toluene and alkanes before being dried and analyzed by diffuse reflectance UV–vis. The absorption spectra of the resulting powders are indicative of the surface Brønsted acidity of the materials, given by an absorption maximum around 550 nm for strong acids ($pK_a < -0.66$), 425–450 nm for medium acids ($0.66 < pK_a < 7.10$), and 620 nm for bases ($pK_a > 7.10$), resulting from the different protonation states of the indicator molecule (Figure 4C). This experiment shows that the Brønsted acidic sites in MIL-100(Al) are medium acids (pK_a comprised between −0.66 and 7.10) and that acidic sites of similar strength are present in the ethylenediamine-functionalized sample (Figure 4D). The experiment also confirms that additionally to those acidic sites, EN@MIL-100(Al) possesses basic sites with a $pK_a > 7.10$ due to the presence of amines, imparting both Brønsted acidity and basicity to this material. The crystallinity of the materials was checked after impregnation with bromothymol blue (see the Supporting Information, Figure S23). Interestingly, crystallinity was maintained for MIL-100(Al), whereas the long-range order in EN@MIL-100(Al) was clearly disrupted after impregnation. Such long-range order disturbance has previously been observed in MIL-100(Al) upon adsorption of other dyes such as methylene blue, Coomassie brilliant blue G-250, and rhodamine B. (45)

CARBON DIOXIDE SORPTION

The adsorption of carbon dioxide in both pristine and functionalized MOFs was studied by means of gravimetric methods at a pressure of 1 atm and by low-pressure adsorption isotherms as well as by volumetric methods at higher pressures. Gravimetric adsorption measurements at 1 atm were performed on a thermogravimetric system in which the samples were first heated at 100 °C under a helium atmosphere to remove physisorbed species but avoid removing or damaging the grafted ethylenediamine. The samples were then cooled down to room temperature, and three adsorption/desorption cycles were performed by switching the working gas from helium to CO_2. The obtained results are shown in the Supporting Information (Figure S24). The results are indicative of the CO_2 sorption kinetics of the materials, as well as their sorption capacity. Concerning the pristine MOFs, MIL-100(Fe) is able to adsorb slightly more carbon dioxide than the aluminum-containing materials, which can be explained by its higher surface area and higher density of open-metal sites

Published in : Inorganic Chemistry (2021), vol. 60, n°21, pp. 16666-16677
DOI: 10.1021/acs.inorgchem.1c02568
Status : Postprint (Author's version)

compared to the other materials. The iron-based MOF also reaches full capacity faster than the two other pristine MOFs, especially during the first adsorption cycle. Upon functionalization with EN, MIL-100(Fe), however, loses its ability to adsorb CO_2, which was expected based on the amorphous nature of the material that was revealed by PXRD and the nonporous nature determined by nitrogen physisorption. EN@MIL-100(Al) adsorbs less CO_2 than its nonfunctionalized counterpart, which can be explained by its lower surface area (smaller free volume of the pores). The bimetallic MOF, however, retains most of its adsorption capacity after functionalization, allowing slightly more CO_2 to be adsorbed in EN@MIL-100(Fe,Al) than in EN@MIL-100(Al). This can be explained by the smaller loss of the surface area of the bimetallic MOF upon functionalization compared to MIL-100(Al). For all of the MOFs, a decrease of gravimetric uptake was observed after functionalization with EN, which is in accordance with a previous report on the functionalization of MIL-100(Cr) with ethylenediamine, (17) but contradictory with another report. (16)

The materials were further investigated by low-pressure gravimetric adsorption experiments (Figure S25). This was done after degassing the samples *ex situ* at 100 °C under vacuum and loading the samples in a TGA system, which was hosted in a glovebox, allowing to avoid the uptake of moisture before the measurement. The samples were then subjected to gas fluxes with variable CO_2/Ar proportions, increasing the partial pressure of CO_2 stepwise. The sample weight was allowed to stabilize between each increase of CO_2 partial pressure by a 30 min equilibration time, after which the weight gain was recorded. Not surprisingly, the adsorption at the highest CO_2 partial pressure (P = 0.8 bar) followed the trends of the gravimetric adsorption experiments at 1 atm. More interestingly, the uptake in the lower partial pressure range is much steeper for EN@MIL-100(Al) than for all other materials. This indicates that this material has a much more marked affinity for CO_2, which can be explained by the interaction of CO_2 with the amine moieties of the MOF. Surprisingly, this feature is absent in the bimetallic counterpart, EN@MIL-100(Fe,Al), indicating that in this material, the amine functions cannot interact with CO_2 as efficiently. When normalizing the adsorbed quantity of CO_2 by the surface area of the materials (Figure S26), the bimetallic MOF seems to be the best performing of all nonfunctionalized MOFs. However, the quantity of adsorbed carbon dioxide by the surface area lowers upon functionalization. After functionalization, EN@MIL-100(Al) absorbs about twice as much CO_2 per square meter than its nonfunctionalized counterpart at partial pressures above 0.25 and about three times more at low partial pressures (P < 0.1 bar), evidencing the higher affinity of the functionalized Al-MOF for CO_2 again upon functionalization with ethylenediamine.

Published in : Inorganic Chemistry (2021), vol. 60, n°21, pp. 16666-16677
DOI: 10.1021/acs.inorgchem.1c02568
Status : Postprint (Author's version)

Volumetric measurements were performed for all of the MOFs displaying porosity (see the Supporting Information, Figure S27) after activation at either 200 °C for nonfunctionalized materials or at 100 °C for the MOFs functionalized with EN. As a general trend, the materials with higher surface areas adsorbed higher quantities of CO_2, the amount adsorbed increases in the following order: EN@MIL-100(Al) [S_{BET} = 657 m^2/g], EN@MIL-100(Fe,Al) [S_{BET} = 839 m^2/g], MIL-100(Fe,Al) [S_{BET} = 1029 m^2/g], MIL-100(Al) [S_{BET} = 1861 m^2/g], and MIL-100(Fe) [S_{BET} = 2048 m^2/g]. At pressures below 25 bar, all of the materials show an adsorption behavior that follows typical Langmuir isotherms (Figure S27). However, it is noticeable that although MIL-100(Fe) follows the Langmuir equation, all of the materials containing aluminum start to absorb an excess of CO_2 compared to what would be expected according to a Langmuir equation above a certain pressure (>25 bar). It is noticeable that the more aluminum the samples contain, the more this deviation from the expected isotherm becomes large. Interestingly, the gas uptake at the pressure point at which the experimental value starts to become different from the expected one shows remarkably slowed down kinetics compared to the ones of the lower pressure points (see Figure 5 for MIL-100(Al) and Figure S28 for other MOFs). Indeed, when following the Langmuir fit, equilibrium is usually reached in about 2 min, whereas during the unexpected increase in uptake, the stabilization takes between 7 and 15 min. Furthermore, those materials display a small hysteresis upon desorption (see the Supporting Information, Figures S29 and 5 for MIL-100(Al)). These observations clearly indicate that some other phenomenon than simple physisorption is occurring in the Al-containing materials. Such behavior is not observed in MIL-100(Fe) and was not reported for any other MIL-100(M) (M = any metal) structure before. (46,47) Calculations (Table S2) show that the deviation from the expected uptake at high pressures is close to one CO_2 molecule per trinuclear cluster for MIL-100(Al) and EN@MIL-100(Al), and roughly half that quantity for MIL-100(Fe,Al) and EN@MIL-100(Fe,Al). This indicates that the presence of aluminum in the material is responsible for the observed effect. As coordinatively unsaturated metal sites are known to be one of the first filled sites during adsorption with coordinating gases like CO_2, and that this adsorption thus occurs at much lower pressures, we ruled out that Al open-metal sites are playing a role in the observed phenomenon. We thus hypothesized that species coordinated to Al are likely undergoing a reversible reaction (chemisorption) with CO_2 at high pressure. We ruled out ethylenediamine and water as the active species, as MIL-100(Al) and MIL-100(Fe,Al) do not contain EN, and the presence of coordinated water in EN@MIL-100(Fe,Al) was ruled out by elemental analysis. The only common species to all of the materials showing the unusual adsorption behavior is thus a hydroxyl moiety coordinated to Al. Based on this observation,

Published in : Inorganic Chemistry (2021), vol. 60, n°21, pp. 16666-16677
DOI: 10.1021/acs.inorgchem.1c02568
Status : Postprint (Author's version)

it can be hypothesized that CO_2 insertion occurs between the oxygen and hydrogen atoms of the hydroxyl moiety. Such behavior can be promoted by the strong polarization of the Al–OH bonds, rendering the hydrogen atoms quite acidic. This mechanism is also in accordance with the fact that the difference between the observed excess uptake and the one expected based on the Langmuir fit is more important for the monometallic Al-based materials than for the bimetallic ones. Indeed, the former contains one Al–OH moiety per cluster, whereas bimetallic Fe,Al materials probably contain a mixture of Al–OH and Fe–OH moieties. This explains why the amount of chemisorbed CO_2 is less than one molecule of carbon dioxide per trimeric cluster for the bimetallic MOFs. Further evidence concerning this adsorption mechanism could be gained from *in situ* spectroscopic characterization (FTIR, NMR, etc.) under high pressure of CO_2. However, these characterization methods require specially dedicated equipment (48) and are thus outside the scope of this work.

Published in : Inorganic Chemistry (2021), vol. 60, n°21, pp. 16666-16677
DOI: 10.1021/acs.inorgchem.1c02568
Status : Postprint (Author's version)

Figure 5

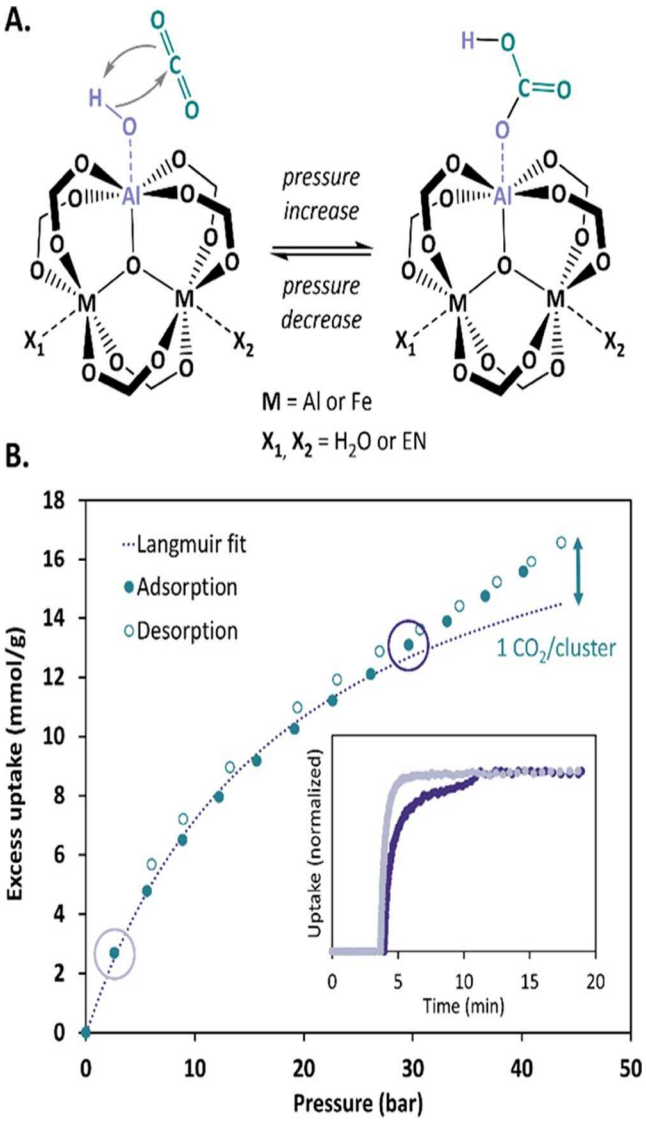

Figure 5. (A) Scheme of the probable mechanism of CO_2 uptake at high pressure in Al-containing MIL-100 MOFs and (B) Experimental sorption isotherm of CO_2 in MIL-100(Al) together with the Langmuir fit and (inset) difference of adsorption kinetics at the 1st and 9th adsorption points (circled on the isotherm), evidencing reaction with CO_2.

Conclusions

We performed functionalization of the metal sites of two distinct monometallic Fe and Al MOFs from the MIL-100 series with ethylenediamine. The second MOF, MIL-100(Al), was obtained under mild conditions as a hierarchically structured solid with micro- and mesopores, free of unreacted trimesic acid, through a new procedure. Our experiments showed that only MIL-100(Al) retains its crystallinity upon reaction with EN, whereas MIL-100(Fe) collapses. These results demonstrate that the choice of the metal composing the MOF's structure is of critical importance for the successful

Published in : Inorganic Chemistry (2021), vol. 60, n°21, pp. 16666-16677
DOI: 10.1021/acs.inorgchem.1c02568
Status : Postprint (Author's version)

functionalization of the metal centers in MOFs rather than the MOF structure. The efficient incorporation of EN in the MOF was demonstrated by an original approach based on solution NMR, allowing us to evidence and quantify the presence of the complete EN molecule, which is not possible using elemental analysis. Solid-state NMR further confirmed that the grafted EN possesses one free $-NH_2$ that adds new functionality to the MOF. The stabilizing role of aluminum in the framework was further demonstrated by reacting EN with a mixed-metal MIL-100(Fe,Al) (Fe/Al = 2/1) MOF, which preserved its crystalline state.

The obtained materials are promising for postfunctionalization through amine chemistry, as demonstrated by the successful reaction with 8-thiomethyl-BODIPY and ninhydrin. Thanks to the reaction with ninhydrin, we were able to demonstrate that the ethylenediamine molecules present in the large diffusion channels of EN@MIL-100(Al), accessible through hexagonal windows of 8.6 Å, can be selectively postfunctionalized by molecules that are too large to diffuse through the smaller diffusion channels formed by the 5 Å-wide pentagonal windows. The amine moieties of the EN in the smaller mesopores (about 59% of the pendant amine sites), only accessible through the small pentagonal windows, can then remain in their pristine state or could be transformed to a different functionality by reaction with a smaller molecule. EN@MIL-100(Al) could thus be used for developing bifunctional materials with a hierarchized distribution of functionalities throughout the framework. Interestingly, EN@MIL-100(Al) possesses both Brønsted acidic and basic sites, as demonstrated by a colorimetric approach based on bromothymol blue adsorption, opening the door to applications such as bifunctional acid/base catalysis. The ethylenediamine-functionalized MOFs show lower gravimetric and volumetric CO_2 uptakes than their pristine counterparts due to the space occupied by the EN molecules, but the functionalization of MIL-100(Al) by ethylenediamine is responsible for a higher affinity of the resulting material toward CO_2 at low partial pressures, as well as higher CO_2 adsorption per surface area, which is promising for gas separation applications. Finally, we evidenced the unusual CO_2 adsorption behavior of aluminum-containing MIL-100 MOFs and their EN-functionalized counterparts, revealing sorption isotherms with an unexpected increase in excess uptake above 25 bar together with slowed down adsorption kinetics and a small hysteretic behavior during desorption, likely ascribed to the formation of carbonate species, which, to the best of our knowledge, is unique among the MOFs of the MIL-100 family.

Published in : Inorganic Chemistry (2021), vol. 60, n°21, pp. 16666-16677
DOI: 10.1021/acs.inorgchem.1c02568
Status : Postprint (Author's version)

Associated content

SUPPORTING INFORMATION

The Supporting Information is available free of charge at https://pubs.acs.org/doi/10.1021/acs.inorgchem.1c02568.

PXRD patterns; FTIR spectra; nitrogen adsorption isotherms; TGA curves and NMR spectra of the pristine and functionalized MOFs; diffuse reflectance spectra of bromothymol blue-adsorbed MOFs and gravimetric and volumetric CO2 sorption curves; and schemes of molecules used for functionalization and diffusion channels in the MOFs as well as calculations and results of elemental analyses (PDF)

AUTHOR CONTRIBUTIONS

This manuscript was written through contributions of all authors. All authors have given approval to the final version of the manuscript.

FUNDING

The authors acknowledge the F.R.S./FNRS for the FRIA fellowship of T.S. and for the grant CdR J.0073.20. We thank Dr S. Ouk for his generous financial support through the Fondation Louvain, that allowed us to acquire a solvent purification system.

NOTES

The authors declare no competing financial interest.

Acknowledgments

The authors acknowledge Dr. François Devred for supplying the reference samples for the bromothymol blue acidity test and Dr. Tommy Haynes for TEM imaging.

Published in : Inorganic Chemistry (2021), vol. 60, n°21, pp. 16666-16677
DOI: 10.1021/acs.inorgchem.1c02568
Status : Postprint (Author's version)

References

1. Senkovska, I.; Barea, E.; Navarro, J. A. R.; Kaskel, S. Adsorptive Capturing and Storing Greenhouse Gases Such as Sulfur Hexafluoride and Carbon Tetrafluoride Using Metal-Organic Frameworks. Microporous Mesoporous Mater. 2012, 156, 115– 120, DOI: 10.1016/j.micromeso.2012.02.021
2. Sumida, K.; Rogow, D. L.; Mason, J. A.; McDonald, T. M.; Bloch, E. D.; Herm, Z. R.; Bae, T. H.; Long, J. R. Carbon Dioxide Capture in Metal-Organic Frameworks. Chem. Rev. 2012, 112, 724– 781, DOI: 10.1021/cr2003272
3. Li, H.; Wang, K.; Sun, Y.; Lollar, C. T.; Li, J.; Zhou, H. C. Recent Advances in Gas Storage and Separation Using Metal–Organic Frameworks. Mater. Today 2018, 21, 108– 121, DOI: 10.1016/j.mattod.2017.07.006
4. Wu, M. X.; Yang, Y. W. Metal–Organic Framework (MOF)-Based Drug/Cargo Delivery and Cancer Therapy. Adv. Mater. 2017, 29, 1606134 DOI: 10.1002/adma.201606134
5. Liu, Y.; Xie, X. Y.; Cheng, C.; Shao, Z. S.; Wang, H. S. Strategies to Fabricate Metal-Organic Framework (MOF)-Based Luminescent Sensing Platforms. J. Mater. Chem. C 2019, 7, 10743– 10763, DOI: 10.1039/c9tc03208h
6. Wang, H. H.; Shi, W. J.; Hou, L.; Li, G. P.; Zhu, Z.; Wang, Y. Y. A Cationic MOF with High Uptake and Selectivity for CO2 Due to Multiple CO2-Philic Sites. Chem. - Eur. J. 2015, 21, 16525– 16531, DOI: 10.1002/chem.201502532
7. Vaidhyanathan, R.; Iremonger, S. S.; Dawson, K. W.; Shimizu, G. K. H. An Amine-Functionalized Metal Organic Framework for Preferential CO 2 Adsorption at Low Pressures. Chem. Commun. 2009, 5230– 5232, DOI: 10.1039/b911481e
8. Ma, W.; Xu, L.; Li, Z.; Sun, Y.; Bai, Y.; Liu, H. Post-Synthetic Modification of an Amino-Functionalized Metal-Organic Framework for Highly Efficient Enrichment of N-Linked Glycopeptides. Nanoscale 2016, 8, 10908– 10912, DOI: 10.1039/c6nr02490d
9. Lin, Y.; Kong, C.; Chen, L. Amine-Functionalized Metal-Organic Frameworks: Structure, Synthesis and Applications. RSC Adv. 2016, 6, 32598– 32614, DOI: 10.1039/c6ra01536k
10. Montoro, C.; García, E.; Calero, S.; Pérez-Fernández, M. A.; López, A. L.; Barea, E.; Navarro, J. A. R. Functionalisation of MOF Open Metal Sites with Pendant Amines for CO 2 Capture. J. Mater. Chem. 2012, 22, 10155– 10158, DOI: 10.1039/c2jm16770k
11. Wang, N.; Mundstock, A.; Liu, Y.; Huang, A.; Caro, J. Amine-Modified Mg-MOF-74/CPO-27-Mg Membrane with Enhanced H2/CO2 Separation. Chem. Eng. Sci. 2015, 124, 27– 36, DOI: 10.1016/j.ces.2014.10.037

12. Zhong, R.; Yu, X.; Meng, W.; Han, S.; Liu, J.; Ye, Y.; Sun, C.; Chen, G.; Zou, R. A Solvent 'Squeezing' Strategy to Graft Ethylenediamine on Cu3(BTC)2 for Highly Efficient CO2/CO Separation. Chem. Eng. Sci. 2018, 184, 85– 92, DOI: 10.1016/j.ces.2017.12.040
13. Yeon, J. S.; Lee, W. R.; Kim, N. W.; Jo, H.; Lee, H.; Song, J. H.; Lim, K. S.; Kang, D. W.; Seo, J. G.; Moon, D.; Wiers, B.; Hong, C. S. Homodiamine-Functionalized Metal-Organic Frameworks with a MOF-74-Type Extended Structure for Superior Selectivity of CO2 over N2. J. Mater. Chem. A 2015, 3, 19177– 19185, DOI: 10.1039/c5ta02357b
14. Choi, S.; Watanabe, T.; Bae, T. H.; Sholl, D. S.; Jones, C. W. Modification of the Mg/DOBDC MOF with Amines to Enhance CO 2 Adsorption from Ultradilute Gases. J. Phys. Chem. Lett. 2012, 3, 1136– 1141, DOI: 10.1021/jz300328j
15. Bai, Z. Q.; Yuan, L. Y.; Zhu, L.; Liu, Z. R.; Chu, S. Q.; Zheng, L. R.; Zhang, J.; Chai, Z. F.; Shi, W. Q. Introduction of Amino Groups into Acid-Resistant MOFs for Enhanced U(vi) Sorption. J. Mater. Chem. A 2015, 3, 525– 534, DOI: 10.1039/c4ta04878d
16. Cabello, C. P.; Berlier, G.; Magnacca, G.; Rumori, P.; Palomino, G. T. Enhanced CO2 Adsorption Capacity of Amine-Functionalized MIL-100(Cr) Metal-Organic Frameworks. CrystEngComm 2015, 17, 430– 437, DOI: 10.1039/c4ce01265h
17. Wang, L.; Zhang, F.; Wang, C.; Li, Y.; Yang, J.; Li, L.; Li, J. Ethylenediamine-Functionalized Metal Organic Frameworks MIL-100(Cr) for Efficient CO2/N2O Separation. Sep. Purif. Technol. 2020, 235, 116219 DOI: 10.1016/j.seppur.2019.116219
18. Sepehrmansouri, H.; Zarei, M.; Ali, M. Multilinker Phosphorous Acid Anchored En / MIL-100 (Cr) as a Novel Nanoporous Catalyst for the Synthesis of New N -Heterocyclic Pyrimido [4, 5- b] Quinolines. Mol. Catal. 2020, 110303 DOI: 10.1016/j.mcat.2019.01.023
19. Pertiwi, R.; Oozeerally, R.; Burnett, D. L.; Chamberlain, T. W.; Cherkasov, N.; Walker, M.; Kashtiban, R. J.; Krisnandi, Y. K.; Degirmenci, V.; Walton, R. I. Replacement of Chromium by Non-Toxic Metals in Lewis-Acid MOFs: Assessment of Stability as Glucose Conversion Catalysts. Catalysts 2019, 9, 437 DOI: 10.3390/catal9050437
20. Bartlett, L.; Vesilind, P. A. Chemistry and Controversy: The Regulation of Environmental Chromium. Environ. Eng. Policy 1998, 1, 81– 86, DOI: 10.1007/s100220050008
21. Férey, G.; Serre, C.; Mellot-Draznieks, C.; Millange, F.; Surblé, S.; Dutour, J.; Margiolaki, I. A Hybrid Solid with Giant Pores Prepared by a Combination of Targeted Chemistry, Simulation, and Powder Diffraction. Angew. Chem., Int. Ed. 2004, 43, 6296– 6301, DOI: 10.1002/anie.200460592
22. Horcajada, P.; Surble, S.; Serre, C.; Hong, D.; Seo, Y.; Chang, J.; Grene, J. Synthesis and Catalytic Properties of MIL-100 (Fe), an Iron (III) Carboxylate with Large Pores. Chem. Commun. 2007, 100, 2820– 2822, DOI: 10.1039/b704325b

Published in : Inorganic Chemistry (2021), vol. 60, n°21, pp. 16666-16677
DOI: 10.1021/acs.inorgchem.1c02568
Status : Postprint (Author's version)

23. Morcombe, C. R.; Zilm, K. W. Chemical Shift Referencing in MAS Solid State NMR. J. Magn. Reson. 2003, 162, 479– 486, DOI: 10.1016/S1090-7807(03)00082-X
24. Bertani, P.; Raya, J.; Bechinger, B. 15N Chemical Shift Referencing in Solid State NMR. Solid State Nucl. Magn. Reson. 2014, 61–62, 15– 18, DOI: 10.1016/j.ssnmr.2014.03.003
25. Steenhaut, T.; Hermans, S.; Filinchuk, Y. Green Synthesis of a Large Series of Bimetallic MIL-100(Fe,M) MOFs. New J. Chem. 2020, 44, 3847– 3855, DOI: 10.1039/d0nj00257g
26. Kim, D.; Ma, D.; Kim, M.; Jung, Y.; Kim, N. H.; Lee, C.; Cho, S. W.; Park, S.; Huh, Y.; Jung, J.; Ahn, K. H. Fluorescent Labeling of Protein Using Blue-Emitting 8-Amino-BODIPY Derivatives. J. Fluoresc. 2017, 27, 2231– 2238, DOI: 10.1007/s10895-017-2164-5
27. Zhang, H.; Wen, J.; Fang, Y.; Zhang, S.; Zeng, G. Influence of Fulvic Acid on Pb(II)Removal from Water Using a Post-Synthetically Modified MIL-100(Fe). J. Colloid Interface Sci. 2019, 551, 155–163, DOI: 10.1016/j.jcis.2019.05.016
28. Mutyala, S.; Yakout, S. M.; Ibrahim, S. S.; Jonnalagadda, M.; Mitta, H. Enhancement of CO2 Capture and Separation of CO2/N2 Using Post-Synthetic Modified MIL-100(Fe). New J. Chem. 2019, 43, 9725– 9731, DOI: 10.1039/c9nj02258a
29. Seoane, B.; Dikhtiarenko, A.; Mayoral, A.; Tellez, C.; Coronas, J.; Kapteijn, F.; Gascon, J. Metal Organic Framework Synthesis in the Presence of Surfactants: Towards Hierarchical MOFs?. CrystEngComm 2015, 17, 1693– 1700, DOI: 10.1039/c4ce02324b
30. Qiu, M.; Guan, Q.; Li, W. Controllable Assembly of Al-MIL-100 via an Inducing Occupied Effect and Its Selective Adsorption Activity. Cryst. Growth Des. 2016, 16, 3639– 3646, DOI: 10.1021/acs.cgd.6b00103
31. Yang, J.; Wang, J.; Deng, S.; Li, J. Improved Synthesis of Trigone Trimer Cluster Metal Organic Framework MIL-100Al by a Later Entry of Methyl Groups. Chem. Commun. 2016, 52, 725– 728, DOI: 10.1039/c5cc08450d
32. Benzaqui, M.; Pillai, R. S.; Sabetghadam, A.; Benoit, V.; Normand, P.; Marrot, J.; Menguy, N.; Montero, D.; Shepard, W.; Tissot, A.; Martineau-Corcos, C.; Sicard, C.; Mihaylov, M.; Carn, F.; Beurroies, I.; Llewellyn, P. L.; De Weireld, G.; Hadjiivanov, K.; Gascon, J.; Kapteijn, F.; Maurin, G.; Steunou, N.; Serre, C. Revisiting the Aluminum Trimesate-Based MOF (MIL-96): From Structure Determination to the Processing of Mixed Matrix Membranes for CO2 Capture. Chem. Mater. 2017, 29, 10326– 10338, DOI: 10.1021/acs.chemmater.7b03203
33. Loiseau, T.; Volkringer, C.; Haouas, M.; Taulelle, F.; Férey, G. Crystal Chemistry of Aluminium Carboxylates: From Molecular Species towards Porous Infinite Three-Dimensional Networks. C. R. Chim. 2015, 18, 1350– 1369, DOI: 10.1016/j.crci.2015.08.006

34. Haouas, M.; Volkringer, C.; Loiseau, T.; Férey, G.; Taulelle, F. Monitoring the Activation Process of the Giant Pore MIL-100(Al) by Solid State NMR. J. Phys. Chem. C 2011, 115, 17934– 17944, DOI: 10.1021/jp206513v
35. Thommes, M.; Kaneko, K.; Neimark, A. V.; Olivier, J. P.; Rodriguez-Reinoso, F.; Rouquerol, J.; Sing, K. S. W. Physisorption of Gases, with Special Reference to the Evaluation of Surface Area and Pore Size Distribution (IUPAC Technical Report). Pure Appl. Chem. 2015, 87, 1051– 1069, DOI: 10.1515/pac-2014-1117
36. Koo, J.; Hwang, I. C.; Yu, X.; Saha, S.; Kim, Y.; Kim, K. Hollowing out MOFs: Hierarchical Micro- and Mesoporous MOFs with Tailorable Porosity via Selective Acid Etching. Chem. Sci. 2017, 8, 6799–6803, DOI: 10.1039/c7sc02886e
37. Jaźwiński, J.; Kamieński, B.; Sadlej, A. Polymeric Adducts of Rhodium(II) Tetraacetate with Aliphatic Diamines: Natural Abundance 13C and 15N CPMAS NMR Investigations. Magn. Reson. Chem. 2013, 51, 788– 794, DOI: 10.1002/mrc.4017
38. Martineau, C.; Taulelle, F.; Haouas, M. The Use of 27Al NMR to Study Aluminum Compounds: A Survey of the Last 25 Years. In The Chemistry of Organoaluminum Compounds (PATAI'S Chemistry of Functional Groups); Micouin, L.; Marek, I.; Rappoport, Z., Eds.; John Wiley & Sons, Ltd.: Chichester, 2016; pp 1– 51.
39. Smith, M. E. Application Of27Al NMR Techniques to Structure Determination in Solids. Appl. Magn. Reson. 1993, 4, 1– 64, DOI: 10.1007/BF03162555
40. Kim, D.; Yamamoto, K.; Ahn, K. H. A BODIPY-Based Reactive Probe for Ratiometric Fluorescence Sensing of Mercury Ions. Tetrahedron 2012, 68, 5279– 5282, DOI: 10.1016/j.tet.2012.01.091
41. Marfin, Y. S.; Usoltsev, S. D.; Rumyantsev, E. V. Decomposition Mechanisms of BODIPY Dyes. In BODIPY Dyes - A Privilege Molecular Scaffold with Tunable Properties; IntechOpen, 2019.
42. Soto-Cantu, E.; Cueto, R.; Koch, J.; Russo, P. S. Synthesis and Rapid Characterization of Amine-Functionalized Silica. Langmuir 2012, 28, 5562– 5569, DOI: 10.1021/la204981b
43. Volkringer, C.; Leclerc, H.; Lavalley, J. C.; Loiseau, T.; Férey, G.; Daturi, M.; Vimont, A. Infrared Spectroscopy Investigation of the Acid Sites in the Metal-Organic Framework Aluminum Trimesate MIL-100(Al). J. Phys. Chem. C 2012, 116, 5710– 5719, DOI: 10.1021/jp210671t
44. Lyle, S. J.; Flaig, R. W.; Cordova, K. E.; Yaghi, O. M. Facilitating Laboratory Research Experience Using Reticular Chemistry. J. Chem. Educ. 2018, 95, 1512– 1519, DOI: 10.1021/acs.jchemed.8b00265
45. Cai, J.; Mao, X.; Song, W. G. Adsorption Behavior and Structure Transformation of Mesoporous Metal-Organic Frameworks towards Arsenates and Organic Pollutants in Aqueous Solution. Mater. Chem. Front. 2018, 2, 1389– 1396, DOI: 10.1039/c8qm00002f

Published in : Inorganic Chemistry (2021), vol. 60, n°21, pp. 16666-16677
DOI: 10.1021/acs.inorgchem.1c02568
Status : Postprint (Author's version)

46. Hamon, L.; Heymans, N.; Llewellyn, P. L.; Guillerm, V.; Ghoufi, A.; Vaesen, S.; Maurin, G.; Serre, C.; De Weireld, G.; Pirngruber, G. D. Separation of CO 2-CH 4 Mixtures in the Mesoporous MIL-100(Cr) MOF: Experimental and Modelling Approaches. Dalton Trans. 2012, 41, 4052– 4059, DOI: 10.1039/c2dt12102f

47. Billemont, P.; Heymans, N.; Normand, P.; De Weireld, G. IAST Predictions vs Co-Adsorption Measurements for CO2 Capture and Separation on MIL-100 (Fe). Adsorption 2017, 23, 225– 237, DOI: 10.1007/s10450-016-9825-6

48. Witherspoon, V. J.; Xu, J.; Reimer, J. A. Solid-State NMR Investigations of Carbon Dioxide Gas in Metal-Organic Frameworks: Insights into Molecular Motion and Adsorptive Behavior. Chem. Rev. 2018, 118, 10033– 10048, DOI: 10.1021/acs.chemrev.7b00695